

# Extended Speed Current Profiling Algorithm for Low Torque Ripple SRM using Model Predictive Control

Siddharth Mehta\*, Md. Ashfanor Kabir<sup>†</sup> and Iqbal Husain\*

\*FREEDM Systems Center, Department of Electrical and Computer Engineering,  
North Carolina State University, Raleigh, NC, USA

<sup>†</sup>ABB US Corporate Research Center, Raleigh, NC, USA  
smehta5@ncsu.edu

**Abstract**—In this work a current profiling algorithm based on semi-numerical model of switched reluctance machine (SRM) is proposed for torque ripple minimization. For extending the low ripple torque control even at higher speeds, the algorithm is developed by keeping both torque ripple and the controller's bandwidth requirements into consideration. The algorithm has a predictive current controller implemented in conjunction with a high accuracy lookup table (LUT) based semi-numerical machine model. A slew rate based analysis shows the effect of the predictive controller's bandwidth on current profile tracking. Simulations are carried out in Matlab/Simulink and results show improved performance with the proposed algorithm at higher speeds than the existing method. As a result, the proposed algorithm provides low ripple torque control opportunity for SRMs over extended speed range.

**Index Terms**—Torque ripple, SRM, MPC, predictive controller, bandwidth analysis, current profiling, current control

## I. INTRODUCTION

Low cost, robustness, and reliability are the driving factors that have pushed SRMs towards industrial adoption [1], but at the same time, these machines have undesirably higher torque ripple [2]. Apart from torque ripple, vibrations and acoustic noise are other major factors inhibiting the widespread use of SRM in high performance applications. Torque ripple heavily depends on the electromagnetic characteristics of the machine. A flatter torque profile in SRM characteristics enables lower torque ripple. However, the most of torque ripple in SRM is contributed during the commutation of a phase, which makes it challenging to develop controllers with high performance [3], [4].

Various techniques can be found in the literature to reduce torque ripple. Several works have been reported in which different type of torque sharing functions (TSFs) are used to indirectly profile the currents for reduced torque ripple [1], [5]. However, TSFs are equation based, and since SRM is a highly nonlinear machine, it is necessary that these TSFs are very accurate to have reduced torque ripple. Therefore, an equation based approach does not prove to be efficient. The reported TSF based profiling techniques still have considerable amount of torque ripple in the range of 20% to 40% at higher speeds, which does not meet the high performance

requirements [5]. On the other hand, the lookup table-based approach of profiling the current has been developed and implemented using a predictive controller in [2], [6]. This approach is highly effective and also suitable from a practical implementation point of view. However, this optimization process does not take the controller capabilities into account, and the current profiles may not be traceable for higher speeds. Similarly, another approach based on differential evolution optimization process is used to profile the currents for torque ripple minimization and vibrations in SRM [3]; however the method is highly complicated. Furthermore, the optimization process does not take the bandwidth of the controller into account. As a result the profiles generated are not optimized for higher speeds. This in turn will affect the torque ripple performance of SRM beyond the base speed.

In this paper, a lookup table based current profiling technique has been implemented. Expressions of the current profile's base angles are calculated considering both torque ripple and controller's bandwidth requirements that help in improving its performance at higher speeds in comparison to the existing method [4]. Bandwidth analysis of the predictive controller is discussed based on slew rate estimation. Moreover, emphasis is given on how this analysis is helpful and plays a major role in designing the current profiles that can be tracked for higher speeds, and thus, provide lower torque ripple for a wider speed range. The paper is divided into four sections. Section II illustrates the profiling method and the bandwidth analysis with a case study based on the proposed algorithm is discussed in Section III, and the work is concluded in Section IV.

## II. PROPOSED CURRENT PROFILING METHOD

In this section, a current profiling technique is proposed keeping both torque ripple as well as the bandwidth of the predictive controller into consideration. A predictive controller is used to track the reference current profiles. These profiles are optimized and designed according to the proposed algorithm which is detailed below. Unlike the conventional controllers such as PI, bandwidth can be obtained from the bode plots using the transfer functions and other conventional control

theory analysis. However, predictive controller predicts the performance that is going to happen in the next few cycles based on the model of the system. There is no tuning of constants for the case of predictive controller. Therefore, the bandwidth of the controller is related to the physical limitations of the control system, such as the sampling frequency, DC bus voltage, switching frequency of the converter and processing time of the digital signal processor. Also, predictive controller is highly dependent on the plant characteristics. In this scenario, SRM is the plant and the phase inductance determines what maximum slew rate a profiled current can have. Hence, the above mentioned factors need to be taken into account while profiling the current.

### A. Slope Estimation

The limitations of the previously proposed current profiling technique in [4] are that the rising and falling slopes of the current were not traceable by the controller at higher speeds. In this algorithm, the emphasis is laid on optimizing the slope of these profiles. First, an initial base profile of the current is designed whose typical shape is shown in Fig. 1. These initial profiles have four major angles,  $\theta_1$ ,  $\theta_2$ ,  $\theta_3$  and  $\theta_4$ .  $\theta_1$  and  $\theta_3$  are indirectly calculated from the rising slope,  $\Delta\theta_{rise}$  and the falling slope,  $\Delta\theta_{fall}$ , respectively in (1) and (2). These calculations heavily depend upon torque and flux characteristics, shown in Figs. 2 and 3, as well as the torque speed envelope of the motor [4].

$$\Delta\theta_{rise} = \frac{L\Delta I\omega}{V_{dc} - I * R - \frac{\delta\lambda}{\delta\theta} * \omega - V_f} \quad (1)$$

$$\theta_2 = \frac{2\pi}{N_R N_{ph}} \quad (2)$$

$$\Delta\theta_{fall} = \frac{L\Delta I\omega}{-V_{dc} - I * R - \frac{\delta\lambda}{\delta\theta} * \omega - V_f} \quad (3)$$

$$\theta_4 = \frac{4\pi}{N_R N_{ph}} \quad (4)$$

Here,  $N_R$  is number of rotor poles,  $N_{ph}$  is the number of phases,  $\omega$  is the maximum speed for which the required torque can be obtained,  $L$  is the aligned inductance,  $V_f$  is the forward diode voltage drop,  $I$  is the flat top current value in the base profile, and  $\Delta I$  is the difference between the flat top current value in the base profile and the minimum value. A typical base profile for 1 N.m command torque with 5% torque ripple and the angular values obtained using the above equations are shown in Fig. 1. While calculating the rising slope, the machine is in the unaligned position although the back electromagnetic force (emf) and the resistive drops are negligible. However, in other instances where the DC Bus voltage is low such as in automotive steering wheel applications where it is 12 V, it is necessary to accommodate the back-emf and the diode voltage drops for proper regulation. Another important consideration is that the falling slope should be greater than the rising slope. It is because during this time the machine is in the aligned position. Hence, the back-emf

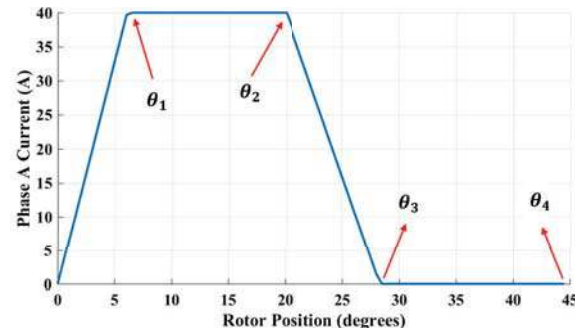


Fig. 1. Initial base current profile.

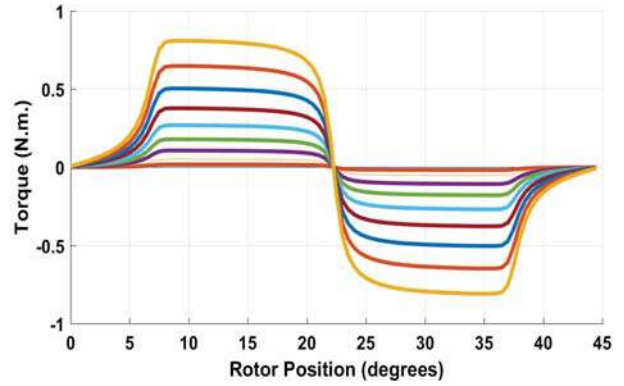


Fig. 2. Torque characteristics of the 12/8 SRM.

voltage drop is very high during this stage of operation. Thus, the phase current requires more time to decrease. Once the base profile has been generated,  $T - I - \theta$  characteristics are used to fine tune the current at each rotor position and then check whether the torque ripple, obtained using the fine-tuned current, is within the tolerance level or not. Once the ripple is within the tolerance level, the next step is to check the slew rate which is explained in the section below. The whole algorithm is summarized in the flow chart in Fig. 4. The other phases are shifted by  $2\pi/(N_R N_{ph})$  degrees mechanically from each other.

### B. Bandwidth Analysis and Slope Verification

For high-performance control, the predictive current controller outperforms conventional control techniques such as hysteresis and PI-based controllers. A hysteresis controller has varying frequency which can add undesirable noise in certain applications, and the PI controller takes several electrical cycles to reach steady state [6]. Meanwhile, the predictive controller is capable of predicting the performance beforehand and adjusting the duty cycle to achieve the current regulation. This makes it very accurate and robust. However, unlike conventional control schemes, the predictive controller does not have a bandwidth term associated with it due to the absence of any designed parameters. The controller is based on the mathematical equations governing the performance of the

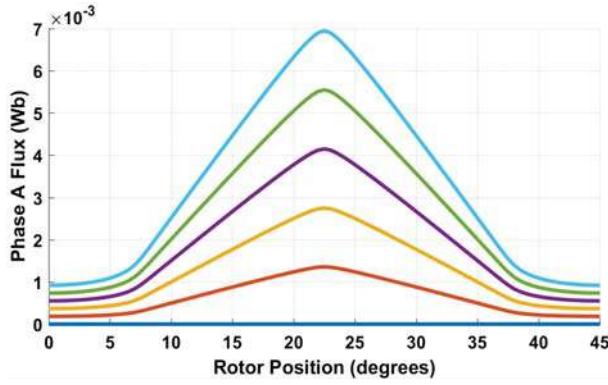


Fig. 3. Flux characteristics of the 12/8 SRM.

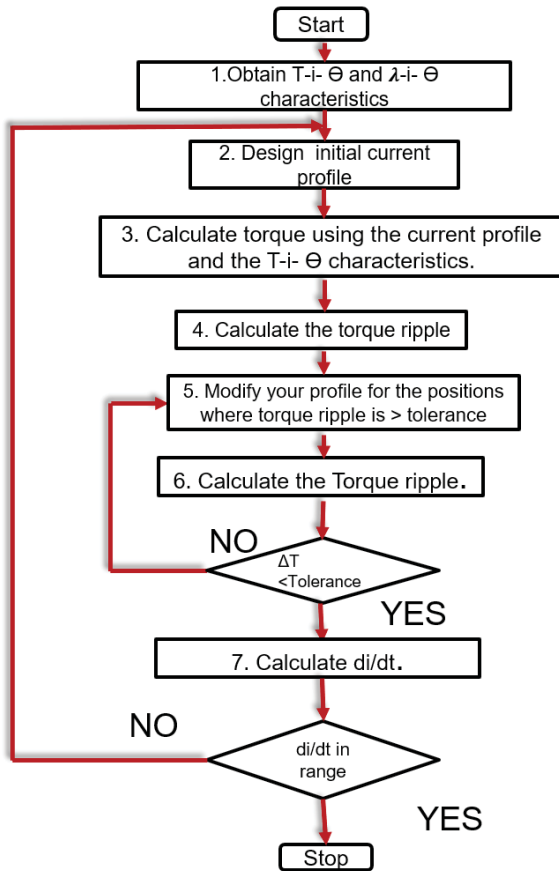


Fig. 4. Flowchart of the proposed algorithm.

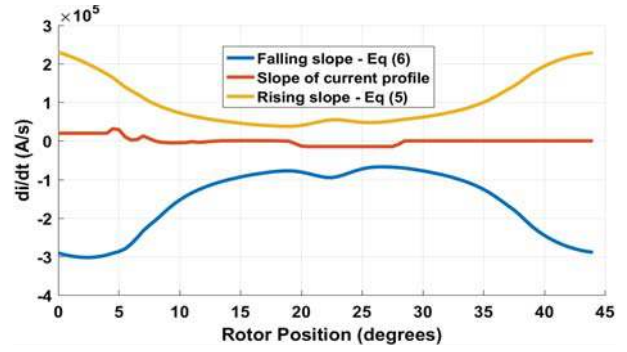


Fig. 5. Current slew rate analysis for 1 N.m at 500 rpm.

model [6]. Hence, the bandwidth of the controller is limited by the physical capabilities of the system. In this case, it is the DC bus voltage, switching frequency, and sampling rate of the current sensor [7] and the plant model which is the SRM in this case. For current profiling technique, the major issue is accurately tracking the slopes of the current especially at high speeds. To overcome this concern, the maximum current rising slew rate and falling slew rate capability at a particular speed are given in (5) and (6), respectively.

$$\frac{di}{dt} = \frac{V_{dc} - IR - \frac{\delta\lambda}{\delta\theta}\omega}{L_{inc}(i, \theta)} \quad (5)$$

$$\frac{di}{dt} = \frac{-V_{dc} - IR - \frac{\delta\lambda}{\delta\theta}\omega}{L_{inc}(i, \theta)} \quad (6)$$

Here,  $L_{inc}$  is the incremental inductance [6]. These two equations represent the maximum allowable slew rate that can be followed at a particular speed,  $\omega$ . Once a current profile is designed using the equations given above, the slew rate of the current profile and the slew rate of the rising current and the falling current are plotted together. If the slew rate of the current profile is out of bounds, then the slopes need to be adjusted using (1) and (3). A representative graph explaining the above scenario is shown in Fig. 5.

### III. RESULTS AND DISCUSSIONS

In this work, the current profiling algorithm has been applied for the design of a 12 V, 3-phase, 12-slot /8 pole SRM. The electromagnetic design and analysis is carried out using finite element analysis (FEA) tool, Altair Flux - 2D; the parameters are given in Table I. This SRM has a peak torque of 2.4 N.m and the base speed is 1000 rpm. In this section, a case study of profiling current with the proposed algorithm is discussed. Currents are profiled for a set torque command of 1 N.m with a maximum torque ripple constraint of 5%. This SRM can achieve 1 N.m upto 1600 rpm only. The machine model is a semi-numerical LUT based model that can be built from FEA data according to [2]; and for current control, the predictive control method has been used [6]. The model considers self flux linkage, while mutual flux linkage has been ignored for this study. In order to show the accuracy of the

proposed profiling method, a comparison is presented between the current profiles designed by the algorithm detailed in [4] and the proposed one. Fig. 6 shows the fine-tuned current profiles according to the proposed method and the current profiling algorithm [4].

TABLE I  
Machine design parameters

Design Variables	Value
Stator outer diameter	85 mm
Rotor outer diameter	52 mm
Rotor inner diameter	10 mm
Stator pole arc angle	15 deg
Rotor pole arc angle	15.5 deg
Stack length	32 mm
Stack yoke length	9.5 mm

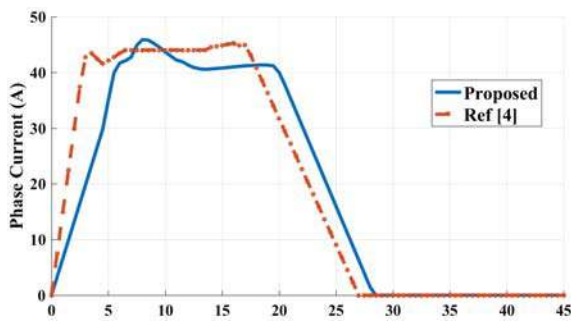


Fig. 6. Profiled currents for 1 N.m torque command

The control angles are calculated using (1)-(4). It can be observed that the currents rate of change is lower in the proposed profiling method than presented in the previous research [4]. To determine the maximum speed up to which these current profiles can be tracked by the controller, the slew rate for both the profiles are shown in Fig. 7 and Fig. 8. It can be observed that in Fig. 7 the slew rate is just within

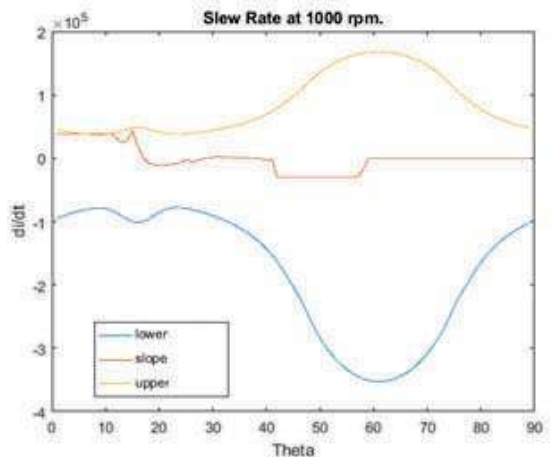


Fig. 7. Slew rate analysis at 1000 rpm for the proposed profiling method.

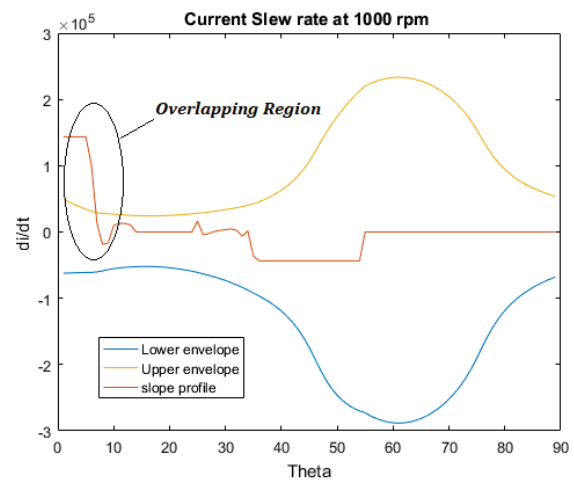


Fig. 8. Slew rate analysis at 1000 rpm for the profiling method in [4].

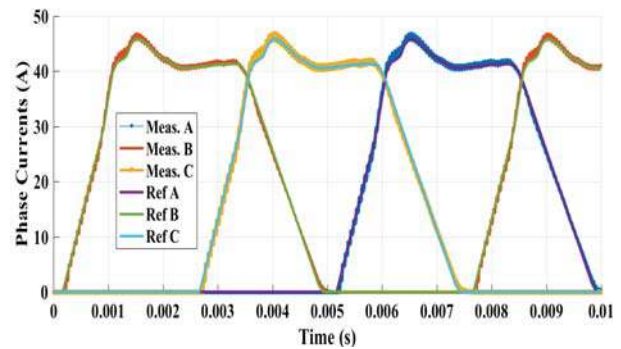


Fig. 9. Phase currents for 1 N.m at 1000 rpm.

the bounds of the upper and lower envelope for 1000 rpm. Whereas the slew rate of the current profile crosses the upper envelope in Fig. 8.

This way of testing predicts that the current profile can be tracked by the controller at 1000 rpm. The same can be observed from the plots shown in Fig. 9. The reference current tracking performance is good and so is the torque

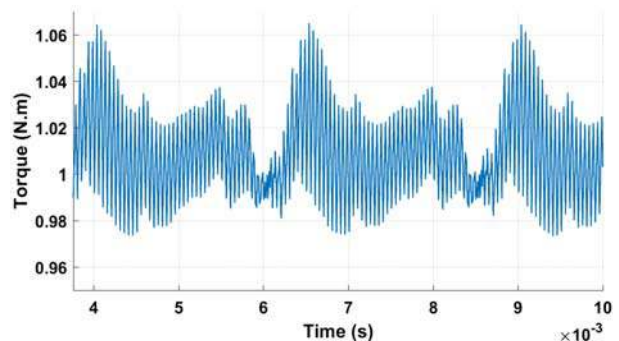


Fig. 10. Torque ripple profile for the profiled currents at 1000 rpm.

ripple performance of the machine as shown in Fig. 10. The torque ripple is 7.5% with the proposed profiling method at 1000 rpm. The same profile is applied at 1500 rpm and the current tracking performance of a single phase is shown in Fig. 11. The major error comes during the magnetization and the demagnetization segments, and the error can be attributed to absence of phase decoupling in the model predictive controller (MPC). During the rise and fall of currents, two phases are active, but the MPC is designed considering that only one phase is operating. Therefore, in order to reduce this error, the improvement has to be achieved from the controller's side. With this performance, the torque ripple is limited to 12%, as shown in Fig. 12. However, the torque ripple performance is still better as compared to [4], as well as to [1] and [5].

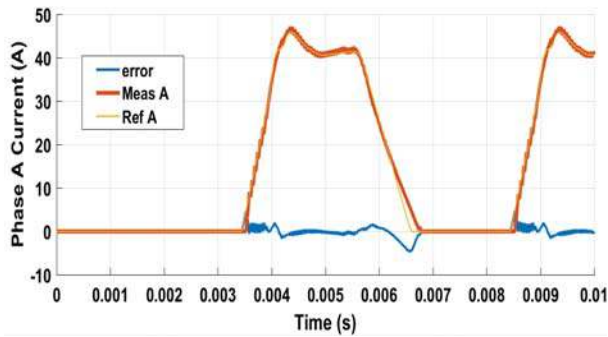


Fig. 11. Reference profile current, measured current and error at 1500 rpm.

To provide additional validation to the previous claims, error analysis had been done in which the root mean square (RMS) error and the peak error is compared between the proposed method and [4]. The RMS error and the peak error analysis is shown in Fig. 13 and Fig. 14. It is clear that with the proposed profiling method, the controller will have a better current tracking performance at higher speeds and will result in better torque ripple performance. For instance, the RMS error for the proposed method is 0.41 A; whereas, the RMS error is 0.59 A for the previous profiling method.

It can be observed with that with the increasing speed the controller has better current tracking performance with the

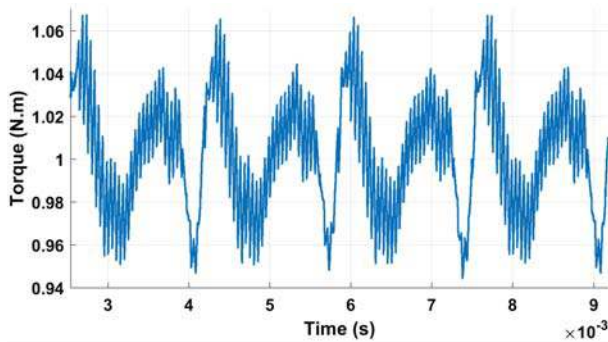


Fig. 12. Torque ripple profile for the profiled currents at 1500 rpm.

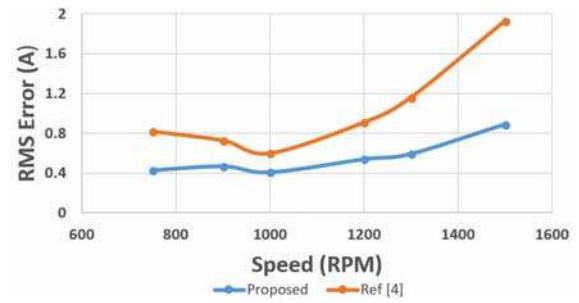


Fig. 13. RMS error analysis with respect to speed.

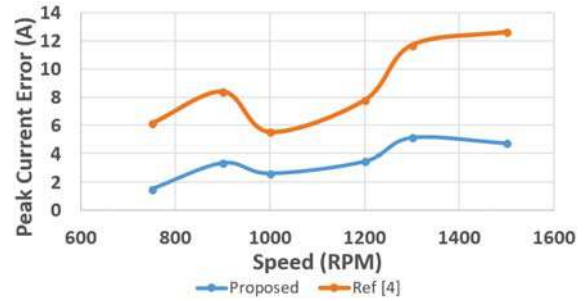


Fig. 14. Peak error analysis with respect to speed.

proposed algorithm as compared to the one in [4]. The peak error analysis in Fig. 14 shows that the peak error for proposed profiling method at 1500 rpm is 4.73 A whereas the peak error for the profiling method in [4] is 12.69 A. The current tracking error reduction is almost 60%. This shows the improvement in the current tracking performance of the controller especially at higher speeds.

#### IV. CONCLUSION

A new SRM current profiling method targeting torque ripple minimization over extended speed range has been proposed. The proposed method implements a LUT based method in which the torque and flux characteristics are required. Model governing the basic shape of the current profile and further tuned based on the torque characteristics has been developed. Bandwidth analysis for a predictive controller is also discussed which is critical for current tracking at the highest operating speeds in addition to meet the torque ripple requirement. The machine model and the predictive controller to track the generated current profile is implemented in the Matlab/Simulink environment. Simulation results for controller performance along with the slew rate analysis at different speeds are shown. Moreover, a comparison in torque ripple performance is presented. These results and analysis confirm that the current profiles generated using the proposed method can be used for higher speeds as compared to existing methods. The RMS error and peak error variation with the speed further shows the effectiveness of this method.

## V. ACKNOWLEDGEMENT

Authors would like to acknowledge the support of Altair for providing the finite element analysis tool Flux 2D.

## REFERENCES

- [1] J. Ye, B. Bilgin, and A. Emadi, "An offline torque sharing function for torque ripple reduction in switched reluctance motor drives," *IEEE Transactions on Energy Conversion*, vol. 30, no. 2, pp. 726–735, June, 2015.
- [2] R. Mikail, I. Husain, and M. Islam, "Finite element based analytical model for controller development of switched reluctance machines," in *2013 IEEE Energy Conversion Congress and Exposition (ECCE)*, Denver, CO, 2013, pp. 920–925.
- [3] C. Ma, L. Qu, R. Mitra, P. Pramod, and R. Islam, "Vibration and torque ripple reduction of switched reluctance motors through current profile optimization," in *2016 IEEE Applied Power Electronics Conference and Exposition (APEC)*, Long Beach, CA, 2016, pp. 3279–3285.
- [4] R. Mikail, I. Husain, Y. Sozer, M. S. Islam, and T. Sebastian, "Torque-ripple minimization of switched reluctance machines through current profiling," *IEEE Transactions on Industry Applications*, vol. 49, no. 3, pp. 1258–1267, May-June, 2013.
- [5] J. Ye, B. Bilgin, and A. Emadi, "An extended-speed low-ripple torque control of switched reluctance motor drives," *IEEE Transactions on Power Electronics*, vol. 30, no. 3, pp. 1457–1470, March, 2015.
- [6] R. Mikail, I. Husain, Y. Sozer, M. S. Islam, and T. Sebastian, "A fixed switching frequency predictive current control method for switched reluctance machines," *IEEE Transactions on Industry Applications*, vol. 49, no. 3, pp. 1258–1267, May-June, 2013.
- [7] H. Dhrimaj, "An evaluation of switched and synchronous reluctance machines for electric power steering application," North Carolina State University, Raleigh, NC, USA, 2016.